

High-strength Steel Sheets Offering High Impact Energy-absorbing Capacity

Akihiro UENISHI¹
Manabu TAKAHASHI¹

Yukihsa KURIYAMA¹

Abstract

Demand for increased impact safety as well as weight reduction of automobiles has increased the use of high-strength steel sheets. The impact energy absorbing capacity of high-strength steel sheets up to 590 MPa was investigated by the finite element method (FEM) analyses in combination with tensile tests at speeds comparable to those of automobile collisions. The FEM analyses show that high dynamic strength and high work hardenability that improves the stability of the buckling process are advantageous in enhancing the impact energy absorbing capacity of automobile parts. TRIP (transformation-induced plasticity) and DP (dual-phase) steels are superior in these properties and suitable for impact energy absorbing components.

1. Preface

Responding to global consciousness of environmental protection, radical improvement of automobile fuel consumption has become a major issue. Typical examples are PNGV (Partnership for a New Generation of Vehicles: development of an 80 miles/gal. car) of the United States and the proposed development of a 100 km/3 lit. car in Europe. To improve fuel consumption it is essential to reduce car body weight, but due to new legal regulations for crash safety in various countries and the pursuit of safety performance by auto manufacturers as a response to user concern, the weight of cars is increasing rather than decreasing.

Under these circumstances 35 steelmakers from 18 countries embarked on a joint development project called ULSAB (Ultra Light Steel Auto Body) in 1994, and in spring 1998 a possibility of a significant body weight reduction by optimum utilization of steel materials was demonstrated in the form of a prototype white body that achieved a 25% weight reduction satisfying crash safety regulations at the same time^{1,2)}. The principal technological elements used therein were wide application of high strength steel sheets and the utilization of the latest production technology such as tailored blank, hy-

dro-form, laser welding, etc. The project revealed the significance of materials on the enhancement of impact energy absorption capacity or crashworthiness.

Many studies on the enhancement of crashworthiness have been carried out via the use of high strength steel sheets³⁾, but various aspects are yet to be clarified about deformation characteristics in a high strain rate range in an actual collision, more than one million times that of usual tensile tests⁴⁾. In an actual crash situation structural members undergo widely varied stress-strain conditions and different strain rates are imposed on different sections of the body structure. For this reason evaluation of the steel material alone is not sufficient and studies of crash behavior as a whole system are also required. The authors therefore made detailed studies of high-speed deformation characteristics of steel sheets and, taking into consideration the results of these studies, also investigated the crashworthiness of structural members by FEM analyses.

This report describes the results of the studies regarding the effects of material properties on the impact energy absorption of axially crushed square tubes, which constitute the principal deformation mode in head-on collisions.

¹ Technical Development Bureau

2. Methods of test and analysis

Table 1 shows chemical compositions and mechanical properties of the high strength steel sheets used as specimens. A high velocity tensile test machine utilizing the one bar method^{5,6)} was used for tests at high strain rates corresponding to the deformation speeds at actual vehicle crash. Generally speaking, the usual load cells commonly used for ordinary tensile tests can not measure the load correctly at high strain rates since stress waves reflected within the load cell are superimposed on the true signals of loads.

Various methods have been proposed to avoid this interference. As shown in Fig.1, the one bar method uses a long output bar as a load cell. Tensile forces are applied to a specimen by a hammer blow and the stress wave travels along the output bar. Because the output bar has a sufficient length, the measurement can be completed before the stress wave reflected at the other end of the output bar returns. In this way the method makes measurements in a strain rate

Table 1 Chemical compositions (mass %) and mechanical properties of the steels

Type of Steel	C	Si	Mn	Ti	Yield strength (MPa)	Tensile strength (MPa)	Elongation (%)
A Mild steel	0.05	0.01	0.24	-	241	348	43
B Solid solution hardened steel	0.08	0.02	1.46	-	370	487	30
C DP steel	0.05	0.89	1.25	-	432	618	27
D Precipitation hardened steel	0.09	0.01	0.80	0.07	539	636	22
E TRIP steel	0.15	1.48	0.99	-	510	644	37

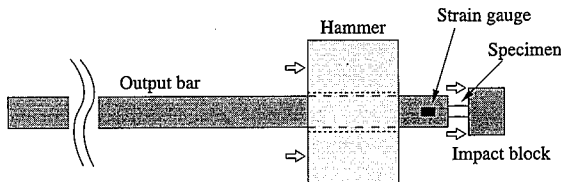


Fig.1 Schematic configuration of one bar type high velocity tensile test machine

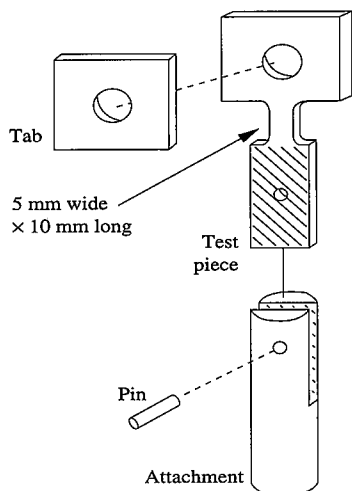


Fig.2 Shape of specimen for high velocity tensile tests

range of 10³/s possible. Fig.2 shows the shape of the specimen. To prevent the dispersion of the stress wave at the interface between the specimen and the output bar, the attachment diameter was made equal to that of the output bar. The test piece was bonded to the attachment with epoxy resin adhesive and it was hardened through a 170°C × 30 min heat treatment, which is virtually equivalent to the painting process conducted in a car assembly line.

An ordinary screw driven test machine was used for tensile tests at strain rates of 10⁻¹ and 10⁻³/s. All the test pieces were of the same shape.

To evaluate the crashworthiness of the structural members, a dynamic explicit (FEM) code was employed for the analyses. A swift type empirical formula was applied for work hardening and Cowper-Symonds' formula⁷⁾ for the effects of strain rate, and thus Equation (1) was derived from these as the material law. Material parameters were obtained by fitting the results of the high-velocity tensile tests to this equation.

$$\sigma(\epsilon, \dot{\epsilon}) = F \cdot (\epsilon + \epsilon_0)^{n*} \cdot \{1 + (\dot{\epsilon}/D)^{1/p}\} \quad (1)$$

where, σ is plastic stress, ϵ is plastic strain, $\dot{\epsilon}$ is strain rate and F , ϵ_0 , D and p are constants. A four-node shell element was used for the analyses.

3. Impact energy absorption characteristics of high strength steel sheets

3.1 Impact energy absorption capacity of high strength steel sheets

Figs.3 and 4 show nominal stress- strain curves of Specimens B and E under strain rates 10³ and 10⁻³/s as examples of high-speed tensile tests. Flow stress showed a rapid increase in the high strain rate range. This tendency was the same with the other steels.

Fig.5 shows the changes of average flow stress of each of the steels in the low strain range (3 - 10%). The mean flow stress value at 10⁻³/s strain rate is shown along the horizontal axis and the same values under 10³/s strain rate are shown along the vertical axis. The dynamic strength of the material increases as static strength goes up but its rate of increase becomes smaller as static strength becomes larger⁶⁾. Among 590 MPa class steels, however, TRIP (transformation induced plasticity) steel and DP (dual phase) steel show larger increases in flow stress under increased strain rates than precipitation-hardened steel. This may be ascribed to the pure ferrite phase existing in both steels. In addition, it is plausible that the accelera-

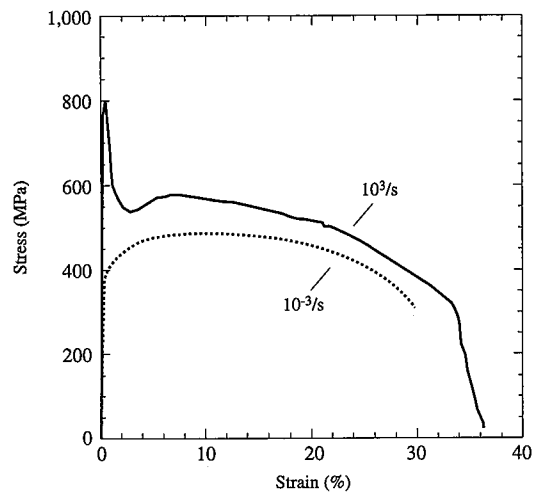


Fig.3 Nominal stress strain curves of specimen B

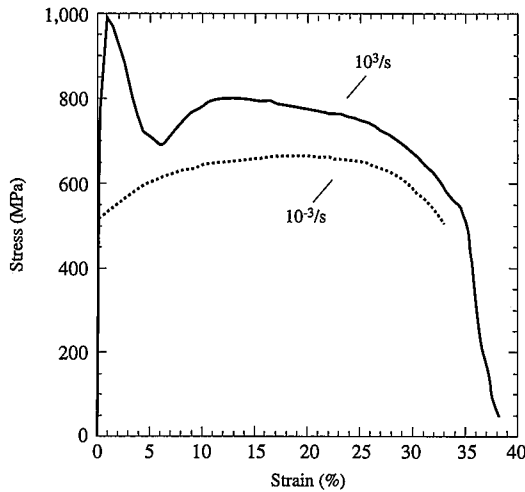


Fig.4 Nominal stress strain curves of specimen E

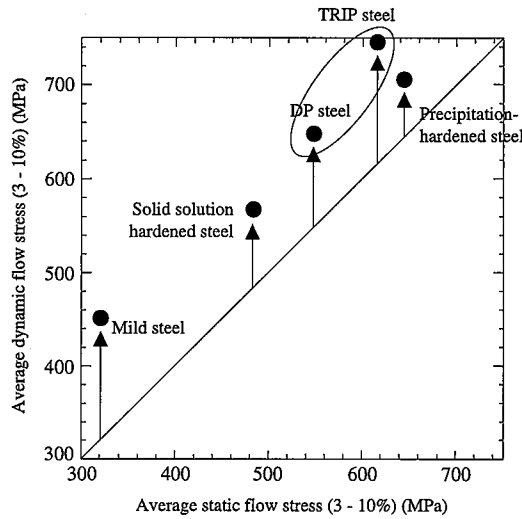


Fig.5 Strain rate-dependency of flow stress

tion of the transformation of retained austenite induced by the increase of flow stress in the ferrite phase also contributes to the observed results in the case of TRIP steel.

The steel material, when used for structural members, undergoes heat treatment during the painting process after the press forming. It is necessary to evaluate its mechanical properties under equivalent conditions in order to understand its performance under actual crash situations⁴. In this meaning, the authors also carried out tensile tests after 5% pre-strain and a heat treatment (170°C × 30 min). The results are shown in Fig.6. Among the 590 MPa class steels, TRIP steel and DP steel show higher dynamic strength in this condition than precipitation-hardened steel. It was also observed that, in the case of DP steel, the pre-strain and the heat treatment contributed to the larger increase in dynamic strength.

Evaluation of crashworthiness of the structural members was carried out by FEM analysis based on the above test results. A square tube (70 mm × 70 mm × 320 mm long, sheet thickness 1.8 mm) was used for the analysis as a simplification of a front side member, which is the main energy absorbing part in a head-on collision. In consideration of the dolly tests (considering a real situation), the tube

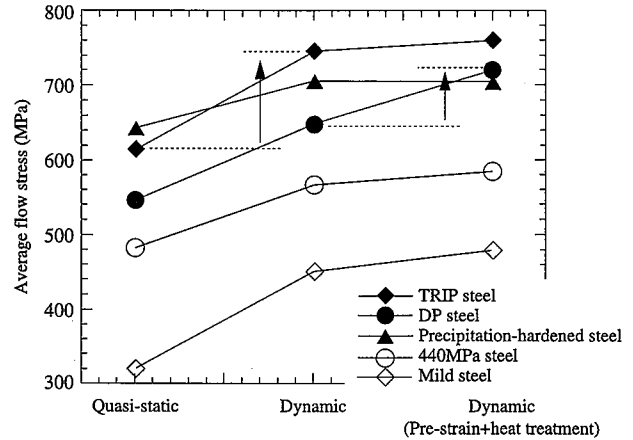


Fig.6 Increase in flow stress by pre-strain

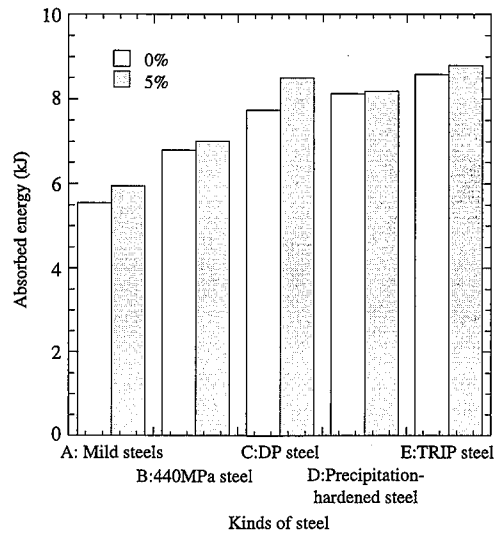


Fig.7 Crashworthiness of square tubes (thickness 1.8 mm)

was made to crush to a rigid wall at an initial velocity of 15 m/s (54 km/h) with a 400 kg weight fixed at the other end of itself.

Fig.7 shows energy absorption of the square tube when it is crushed up to 100 mm axially. The figure shows the energy absorption of materials pre-strained at 0% and 5%. It was observed that the crashworthiness increases by material substitution and the absorbed energy increases by about 40% when mild steel was substituted with 590 MPa class steel. Different kinds of 590 MPa class steels shows different energy absorption capacities depending on the hardening mechanism: TRIP steel and DP steel absorbed more energy than precipitation-hardened steel under the 5% pre-strain condition, which corresponds to the actual energy absorption situation of the structural members. This fact reflects the results shown in Fig.6, i.e. by increasing the strain rate-dependency of flow stress and the effects of pre-strain, a better energy absorption capacity can be given to the structural member even when quasi-static strength of the steels is same. As TRIP steel and DP steel are superior in these properties, a higher energy absorption performance can be expected by the use of these steels for the structural members.

3.2 Effects of material characteristics on collapse mode

In the tests described in the previous section, comparative studies of materials were carried out under a set of conditions where

stable buckling mode was occurred for the purpose of clarifying the energy absorption capacity of the materials. When the sheet thickness is small compared to the section size of the member, however, the collapsing mode will not always be stable^{8,9}. Fig.8 shows the results of dynamic crush tests of members having different thicknesses¹⁰. Where the thickness is small, a collapse mode called the non-compact mode⁸ can take place wherein there remain some portions that hardly take part in the deformation of the side walls. It is supposed that this is caused by local concentration of deformation from the low bending moment due to the small sheet thickness, but the effects of the material properties on this phenomenon are not clear.

For the purpose of investigating the effects of yield strength and work-hardenability of the material in the plastic region, the authors made analyses using the sets of virtual material properties shown in Fig.9. The investigation was carried out under a condition where the non-compact collapse mode was likely to occur, i.e. material thickness/side wall width = 0.8 / 7.0 = 0.011. Fig.10 shows the collapsed shapes of the three cases shown in Fig.9 after 7 minutes had elapsed

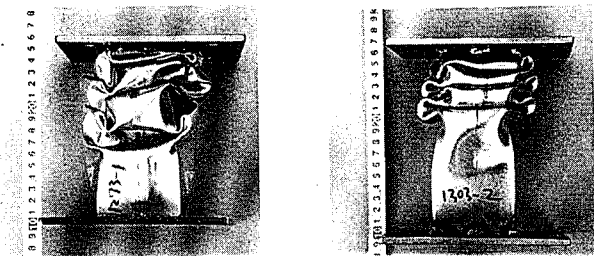


Fig.8 Difference of collapsed shape depending on the thickness of tubes (Left: 0.75 mm, Right: 1.8 mm)

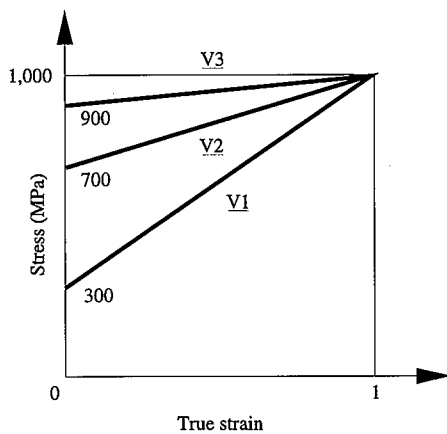


Fig.9 Virtual material properties for analyses

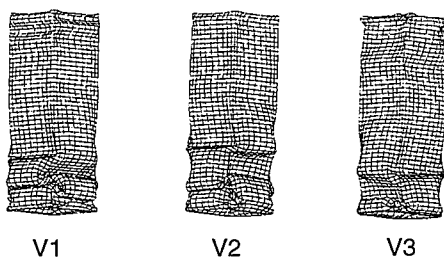


Fig.10 deformed shapes of square tubes

from the start of the collision. Whereas the non-compact mode is suppressed in V1 with high work-hardenability material, it is observed in V3 a material having low work-hardenability. It was conventionally supposed that the local buckling load which causes the non-compact mode was smaller than yield strength of the material and that a geometrical factor (material thickness/side wall width) was the main cause, material characteristics (behavior in the plastic region, among others) were barely considered. In this study, however, clarification of the fact that the non-compact mode is better suppressed when the work-hardenability of the material is higher was made.

Further, to examine the effects of material properties on the stability of the buckling process, other analyses were carried out where the direction of the impact was slanted by 2°. The results are shown in Fig.11. The square tube showed non-compact behavior transitions from axial collapse to bending collapse at the slanted impact, whereas other tubes did not show such a transition.

Some parts of automobile structures actually have a small thickness relative to the sectional size and it is rare that the impact energy is imposed precisely in the axial direction during a crash. Since the energy absorption capacity of bending collapse is smaller than axial collapse, decreased crashworthiness of certain parts due to the early transition to bending collapse might change the crash behavior of the whole body structure into an unpredictable realm. In order to avoid this, it is important, therefore, to suppress the occurrence of the non-compact mode for energy absorbing parts and stabilize the progress of buckling. One of the ways to realize this would be to use materials having high work-hardenability. Fig.12 shows changes to the n-value under dynamic tensile tests¹¹. It is clear that TRIP steel and DP steel have superior work-hardenability among the 590 MPa class steels, and the use of these steels is considered to be effective for improving the stability of the collapsing process.

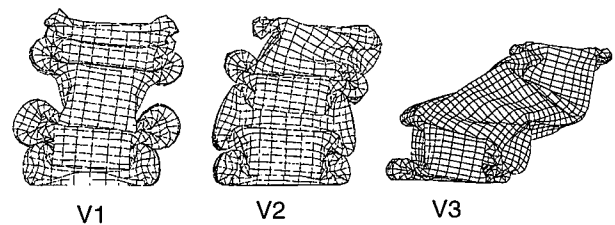


Fig.11 Deformed shapes under slanted load

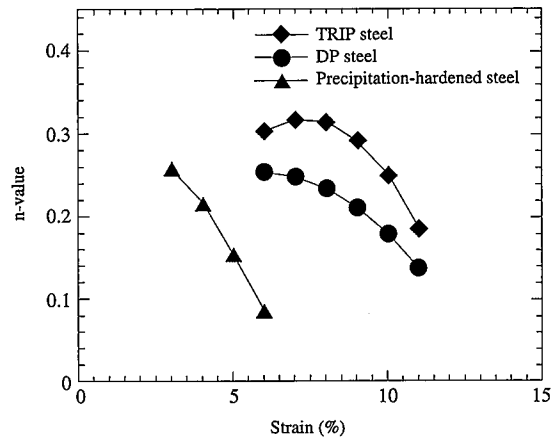


Fig.12 Strain-dependency of n-value under dynamic tensile tests

3.3 Provisional estimation of body weight reduction by the use of high strength steel sheets

It has been clarified that high strength steel sheets have a better impact energy absorption capacity than mild steel, but to reduce body weight it is essential that superior performance is maintained when the thickness of the material is reduced. Accordingly, the authors then studied the effects of material thickness on crashworthiness. Fig.13 shows the plastic strain distribution in a 70 mm side of a square tube made by steel B after collapse. Plastic strain at each position was calculated by averaging plastic strain in the collapsed portion along the crushing direction. From this figure it is understood that a thickness increase would result in (1) stronger constraints at the corners and (2) increase of bending strain in the center of the side wall. It is also understood that the average plastic strain imposed by the crush was 10 - 15%, and hence the flow stress of the materials in the lower strain region is important.

Fig.14 shows the thickness-dependency of absorbed energy (with 5% pre-strain) at a 100 mm crash distance obtained from analyses, changing the sheet thickness from 0.8 to 2.0 mm. Although the difference in energy absorption capacity between the materials is small in the small gauge range it become evident that sheet thickness can be reduced when the steel materials having superior characteristics are used.

The following equation concerns the thickness-dependency of energy absorption capacity of square tubes^{12,13}.

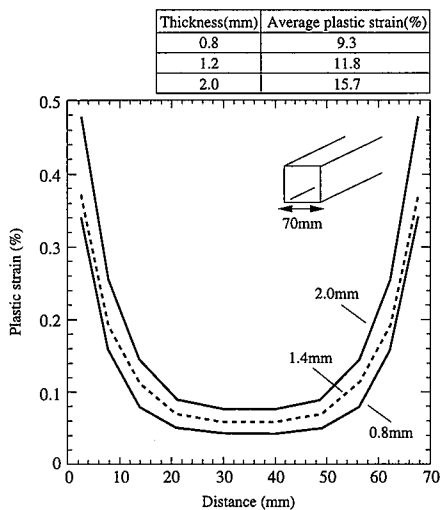


Fig.13 Strain distribution of square tube after crush

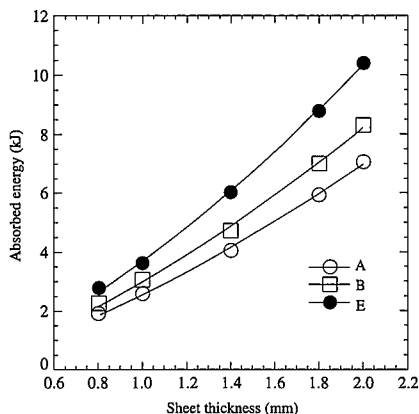


Fig.14 Thickness-dependency of absorbed energy(with 5% pre-strain)

$$E_{ab} = C\delta L^{1/3} t^{5/3} \quad (2)$$

Where, L is side wall width, δ is stroke of crush, t is sheet thickness and C is a constant. The thickness-dependency of absorbed energy calculated from the above equation is shown as solid line curves in Fig.14. As seen here the calculated figures are highly concordant with the results of the analyses and Equation (2) proved to be suitable for expressing the absorbed energy. It is known that the value of C is proportional to the dynamic strength of the material¹³, which indicates that it is important to use high strength materials having high dynamic strength. The results show that, for the square tube used here, 2.0 mm thick mild steel (Specimen A) and 2.0 mm thick 440 MPa steel (Specimen B) can be substituted with 1.6 mm and 1.8 mm sheets, respectively, of 590 MPa TRIP steel (Specimen E), achieving 20% and 10% thickness (=weight) reductions, respectively.

4. Conclusion

Environmental protection, and reduction of CO₂ emissions to prevent global warming among others, have become important issues and the necessity for fuel economy in automobiles has become more and more pronounced. In some respects, improvement of crash safety contradicts with the reduction of car body weight, which is essential for reducing fuel consumption. However, with material substitution there is the possibility of realizing both enhancement of crashworthiness and reduction of weight. In the ULSAB, application of 590 MPa class steel was limited to comparatively "easy-forming" parts, since global availability of materials was one of the prerequisites of the project and, the limited variety of materials thus imposed, high strength and high formability materials could not be counted on. The TRIP steel and DP steel described here have high impact energy absorption capacity as well as excellent formability¹⁴ and they are expected to expand applications to the sections the conventional high tensile steels could not be used for due to their poor formability.

Development of yet more superior materials will be a natural course of events as requirements for car body materials become more and more demanding, and development of application technologies for the newly developed materials will also become essential. It is hoped that lighter car bodies having yet higher safety performance against impact will be realized through the pursuit of the potential of steel for weight reduction to the extreme.

References

- 1) Kuriyama, Y.: J. JSTP. 39 (453), 1009 (1998)
- 2) Hashimoto, K. et al.: '98 Spring Meeting, The Society of Automobile Engineers of Japan, 1998, p.1
- 3) Takechi, H. et al.: Int. J. of Vehicle Design, IAVD Congress on Vehicle Design and Components. Z1, 1984
- 4) Uenishi, A. et al.: International Body Engineering Conference. No.23, 1996, p.89
- 5) Kawata, K. et al.: Mechanical Properties at High Rates of Strain 1979, ed. J. Harding, Institute of Physics, Conference Series
- 6) Nakanishi, E. et al.: Structural Failure, Product Liability and Technical Insurance. 1992, p.423
- 7) Cowper, G.R. et al.: Brown Univ. Div. of Applied Mech. Report No.28, 1952
- 8) Reid, S.R. et al.: Int. J. Mech. Sci. (28), 295 (1986)
- 9) Uenishi, A. et al.: 74th Annual Meeting of Japan Soc. Mechanical Eng. (II), 96-15, 1996, p.449
- 10) Uenishi, A. et al.: International Body Engineering Conference, No.29, 1997, p.59
- 11) Takahashi, M. et al.: International Body Engineering Conference, No.29, 1997, p.26
- 12) Wierzbicki, T. et al.: J. Apl. Mech. (50), 72 (1983)
- 13) Uenishi, A. et al.: '97 Spring Meeting, JSTP, 1997, p.179
- 14) Hiwatashi, S. et al.: 26th International Symposium on Automotive Technology and Automation, 1993, p.263